PROCEEDINGS OF SCIENCE

Isolated photon production in the color dipole picture

Yuri N. Lima,[a,*] **Victor P. B. Gonçalves,**[a] **Roman Pasechnik**[b,c] **and Michal Šumbera**[c]

[a] *Instituto de Física e Matemática, Universidade Federal de Pelotas - UFPEL, 96010-900, Pelotas, Brasil*

[b] *Department of Astronomy and Theoretical Physics, Lund University, SE-223 62, Lund, Sweden*

[c] *Nuclear Physics Institute of the CAS, 25068, Řež, Czech Republic*

E-mail: limayuri.91@gmail.com, barros@ufpel.edu.br, roman.pasechnik@thep.lu.se, sumbera@ujf.cas.cz

A phenomenological study of the isolated photon production in high energy pp and pA collisions at RHIC and LHC energies is performed. Using the color dipole formalism, we investigate the impact of the saturation effects on the production cross sections considering three different phenomenological models for the universal dipole cross section. Predictions for the rapidity dependence of the ratio of pA to pp cross sections are also presented. Moreover, we present our predictions for the correlation function in azimuthal angle $\Delta\phi$ between the photon and a forward pion for different energies and photon rapidities. Our results demonstrate that the presence of saturation effects implies a double-peak structure in the correlation function around $\Delta\phi \simeq \pi$ when the isolated photon and the pion are produced at forward rapidities.

XV International Workshop on Hadron Physics (XV Hadron Physics) 13 -17 September 2021
Online, hosted by Instituto Tecnológico de Aeronáutica, São José dos Campos, Brazil

*Speaker

PoS(XVHadronPhysics)076

1. Introduction

The isolated photon production in pp and pA high-energy collisions is a clean probe for strong interactions in the perturbative regime of Quantum Chromodynamics (QCD). As in the the Drell-Yan (DY) pair production, the isolated photon production at high-p_T provide efficient means for phenomenological analysis of various nuclear effects. Our focus in this contribution is the isolated photon production off the proton and nuclear targets in the low-x regime of QCD in the framework of the phenomenological color dipole formalism. In the high-energy, the projectile quark effectively probes a dense gluonic field in the target, which implies that the isolated photon production cross section is strongly sensitive to the presence of nonlinear effects in the QCD dynamics.

In this contribution we will summarize the results presented in Ref. [1]. In particular, we will present our predictions for the transverse momentum distribution of isolated photons produced at the RHIC and LHC and for the ratio between the proton-lead (pPb) and proton-proton (pp) cross sections at the LHC. Moreover, results for the azimuthal correlation between the photon and a pion that emerges from a projectile quark hadronization will also be presented.

2. Isolated photon production

In the color dipole formalism, the differential cross section for the real photon production is given by

$$\frac{d\sigma(pT \to \gamma X)}{d^2p_T d\eta} = \frac{2p_T}{\sqrt{s}}\cosh(\eta)\frac{x_1}{x_1+x_2}\sum_f \int_{x_1}^1 \frac{d\alpha}{\alpha^2}[q_f(x_1/\alpha,\mu_F^2)+\bar{q}_f(x_1/\alpha,\mu_F^2)]\frac{d\sigma^f(qT\to q\gamma X)}{d\ln\alpha d^2p_T}, \quad (1)$$

where p_T and η are the transverse momentum and pseudorapidity of the emitted photon, $\sqrt{s}$ is the center - of - mass energy and the Feynman variable is defined by $x_F \equiv x_1 - x_2$, with $x_1 = (p_T/\sqrt{s})e^{\eta}$, $x_2 = (p_T/\sqrt{s})e^{-\eta}$. Moreover, $q_f(\bar{q}_f)$ are the unpolarized projectile quark (antiquark) collinear PDFs associated to (valence and sea) flavor $f = u, d, s, c$, which depend of the momentum fraction of the projectile quark taken from the parent nucleon $x_q = x_1/\alpha$. The QCD factorization scale is assumed to be $\mu_F = p_T \equiv |\mathbf{p}_T|$. The differential cross section of the high-p_T real photon production in the quark-target scattering subprocess is represented in the dipole picture as

$$\begin{aligned}\frac{d\sigma^f(qT\to q\gamma X)}{d\ln\alpha d^2p_T} = \frac{1}{(2\pi)^2}\int d^2\rho_1 d^2\rho_2 e^{i\mathbf{p}_T\cdot(\boldsymbol{\rho}_1-\boldsymbol{\rho}_2)}\Psi(\alpha,\boldsymbol{\rho}_1,m_f)\Psi^*(\alpha,\boldsymbol{\rho}_2,m_f)\\ \times\frac{1}{2}[\sigma^T_{q\bar{q}}(\alpha\boldsymbol{\rho}_1,x_2)+\sigma^T_{q\bar{q}}(\alpha\boldsymbol{\rho}_2,x_2)-\sigma^T_{q\bar{q}}(\alpha|\boldsymbol{\rho}_1-\boldsymbol{\rho}_2|,x_2)],\end{aligned} \quad (2)$$

where m_f is the constituent quark mass and $\Psi(\alpha,\boldsymbol{\rho},m_f)$ is the LC wave function of the real photon radiation off a quark with flavor f. The quark-γ transverse separations amplitude and its conjugate are considered to be different and are denoted as $\boldsymbol{\rho}_{1,2}$. Following Ref. [2], we take $m_u = m_d = m_s = 0.14$ GeV and $m_c = 1.4$ GeV. The overlap of the photon bremsstrahlung wave functions in Eq. 2, summed over the transverse polarizations of the radiated hard photon, reads

$$\Psi(\alpha,\boldsymbol{\rho}_1,m_f)\Psi^*(\alpha,\boldsymbol{\rho}_2,m_f) = \frac{\alpha_{em}e_f^2}{2\pi^2}\left\{m_f^2\alpha^4K_0(\tau\rho_1)K_0(\tau\rho_2)+[1+(1-\alpha)^2]\tau^2\frac{\boldsymbol{\rho}_1\cdot\boldsymbol{\rho}_2}{\rho_1\rho_2}K_1(\tau\rho_1)K_1(\tau\rho_2)\right\}, \quad (3)$$

where $\bar{\alpha} \equiv 1 - \alpha$, α_{em} is the fine structure constant, e^f is the charge of the projectile quark, $\rho_{1,2} \equiv |\boldsymbol{\rho}_{1,2}|$, $\tau = \alpha m_f$, and the modified Bessel functions of the second kind are denoted as $K_{0,1}$.

One of the important observables sensitive to the dynamics of saturation is the correlation function $C(\Delta\phi)$ in azimuthal angle $\Delta\phi$ between the final state photon and hadron, which is defined by

$$C(\Delta\phi) = \frac{2\pi \int_{p_T, p_T^h > p_T^{cut}} dp_T\, p_T\, dp_T^h\, p_T^h \frac{d\sigma(pT \to h\gamma X)}{d\eta dy_h d^2p_T d^2p_T^h}}{\int_{p_T > p_T^{cut}} dp_T\, p_T \frac{d\sigma(pT \to \gamma X)}{d\eta d^2p_T}}, \tag{4}$$

in terms of the low cutoff p_T^{cut} on transverse momenta of γ and h. In the denominator, we have the cross section for inclusive photon production in association with a leading hadron h, which is given by

$$\frac{d\sigma(pT \to h\gamma X)}{d\eta dy_h d^2p_T d^2p_T^h} = \frac{\alpha_{em}}{2\pi^2} \int_{\frac{x_h}{1-x_1}}^1 \frac{dz_h}{z_h^2} \sum_f e_f^2 D_{h/f}(z_h, \mu_F^2) x_p q_f(x_p, \mu_F) S_\perp F_T(x_g, k_T^g) \frac{\bar{z} z^2 (1 + \bar{z}^2) k_T^{g2}}{P_T^2 (\mathbf{P}_T + z\mathbf{k}_T^g)^2}, \tag{5}$$

where the key kinematical variables are determined as: $x_h \simeq (p_T^h/\sqrt{s})e^{yh}$, $x_p = x_1 + x_h/z_h$, $z = x_1/x_p$, and $x_g = x_1 e^{-2\eta} + (x_h/z_h)e^{-2y_h}$; and also $\mathbf{k}_T^g = \mathbf{p}_T + \mathbf{k}_T^q$, $\mathbf{P}_T = \bar{z}\mathbf{p}_T - z\mathbf{k}_T^q$, and $\mathbf{k}_T^q = \mathbf{p}_T^h/z_h$. Moreover, $D_{h/f}$ is the fragmentation function of the projectile quark q_f into a final-state (light) hadron h carrying $\mathbf{p}_T^h$, y_h is the rapidity of the hadron h in the final state, z_h and x_h are respectively the LC momentum fractions taken by the hadron h from the parent quark q_f and the incoming proton, $\mathbf{P}_T$ is the relative transverse momentum between the photon and the quark q_f, $\mathbf{k}_T^q$ is the transverse momentum of the projectile quark q (before fragmenting), $\mathbf{k}_T^g$ is the transverse momentum of the exchanged gluon in the t channel, $S_\perp$ is the transverse area of the considered target T, and $F_T(x_g, k_T^g)$ is the Unintegrated Gluon Distribution Function (UGDF) in the target T.

For the numerical analysis, we consider three different phenomenological models for the cross section of the dipole: the Golec-Biernat–Wusthoff (GBW) model [2] relying on a simple saturated ansat; a solution of the Balitsky-Kovchegov equation [3, 4] with running coupling obtained in Ref. [5] denoted as AAMQS; and a phenomenological saturation model based upon the color glass condensate (CGC) approach [6]. In the case of a heavy nucleus target we will assume the Glauber-Mueller (GM) approach [7, 8] based upon resummation of all the multiple elastic rescattering diagrams.

3. Results

In Figs. 1 (a) and (b) we present our predictions for the isolated photon production in pp collisions at $\sqrt{s} = 14$ TeV and two values for the photon pseudorapidity, $\eta = 4$ and $\eta = 6$. The AAMQS prediction yields a higher spectrum than the other models, particularly, at large photon transverse momenta while the CGC and GBW parametrizations provide similar predictions. Note that at small p_T, however, the AAMQS prediction becomes slightly below the GBW one. The impact of nuclear effects on the production of isolated photons in pPb at the LHC can be estimated by calculating the nuclear modification factor $R_{pA} = \sigma_{pA}/A\sigma_{pp}$. The associated results are presented in Fig. 1 (c). Our predictions use the GM approach for the dipole-nucleus cross section and also a solution of the BK equation (called rcBK). We can note that the GM model predicts that the

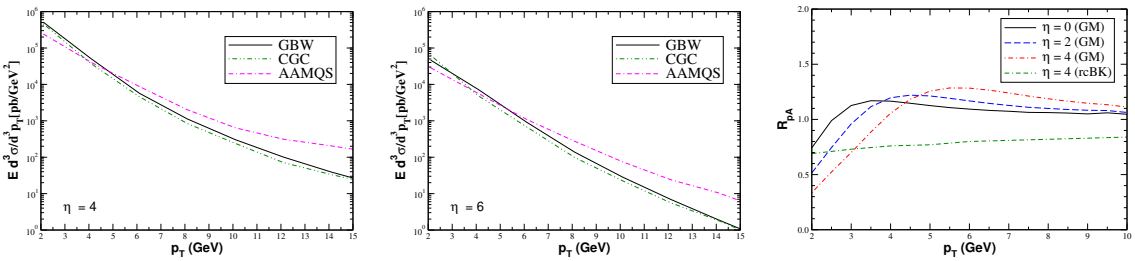

(a) (b) (c)

Figure 1: Isolated photon transverse-momentum spectra in pp collisions at $\sqrt{s}$ = 14 TeV of the LHC experiments for (a) $\eta = 4$ and (b) $\eta = 6$. (c) Transverse momentum dependence of the normalized nuclear modification factor R_{pA} for isolated photon production in pPb collisions ($A = 208$) at the LHC ($\sqrt{s}$ = 8.8 TeV) for several selected values of the photon pseudorapidity η and for two distinct (GM and rcBK) models of the dipole-nucleus cross section.

factor R_{pA} becomes smaller than one for small values of p_T, and the transition depends on the pseudorapidity and shifts to larger values of p_T when we consider larger values of η. For rcBK, we notice that R_{pA} is below one in the entire p_T range considered.

Our predictions for the correlation function $C(\Delta\phi)$, defined in Eq. 4, considering the production of isolated photons and pions at the LHC in pp and pPb collision are presented in Fig. 2. The calculations were performed using the GBW model. The results presented in Fig. 2 (a) and (b) indicate that the single peak red line (back-to-back correlation) gives way to a double peak structure when we consider higher pseudorapidity values. The presence of a double peak with a dip in $\Delta\phi = \pi$ is a direct manifestation of the saturation physics. We can also note that the decorrelation is even greater for the pPb case (blue lines) than for the pp case (red lines). In Fig. 2 (c) we analyze the impact of atomic mass on the correlation function in pPb collisions. One has that the decorrelation increases for heavier nuclei, which is directly associated to the atomic number dependence of the saturation scale. Similar results are obtained for RHIC energies (for details, see Ref. [1]).

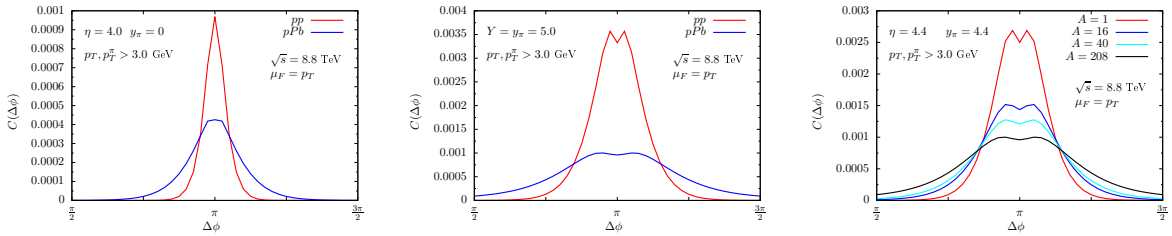

(a) (b) (c)

Figure 2: (a) and (b) Predictions for the correlation function $C(\Delta\phi)$ considering the associated photon and pion production in pp and pPb collisions at the LHC ($\sqrt{s}$ = 8.8 TeV) considering distinct configurations for the isolated photon and pion rapidities. (c) Atomic number dependence of the correlation function $C(\Delta\phi)$ for the associated photon and pion production in pA collisions at the LHC ($\sqrt{s}$ = 8.8 TeV).

4. Summary

In this contribuition, we provide a brief overview of our phenomenological analysis of the isolated photon production in pp and pA collisions at typical RHIC and LHC energies in the framework of the color dipole approach. We employed three different phenomenological saturation models for the dipole-target scattering. Besides, we have investigated the correlation function $C(\Delta\phi)$ in the azimuthal angle between the real high-p_T photon produced in association with a leading pion emerging via fragmentation of a projectile quark which emits the photon. This observable has been studied in pp and pA collisions at RHIC and LHC energies and at different rapidities of final states. In pp collisions, the correlation function exhibits a double-peak structure close to $\Delta\phi \simeq \pi$ in certain kinematical configurations corresponding to both the real high-p_T photon and the accompanied high-p_T pion being produced at forward rapidities. In the case of pA collisions, a larger nuclear saturation scale enforces a stronger decorrelation between the photon and the pion.

Acknowledgements

This work was partially financed by the Brazilian funding agencies CNPq, CAPES, FAPERGS and INCT-FNA (process number 464898/2014-5).

References

[1] V. P. Goncalves, Y. Lima, R. Pasechnik, and M. Šumbera, *Isolated photon production and pion-photon correlations in high-energy pp and pA collisions*, *Phys. Rev. D* **101** (2020) 094019.

[2] K. Golec-Biernat and M. Wüsthoff, *Saturation effects in deep inelastic scattering at low Q^2 and its implications on diffraction*, *Phys. Rev. D* **59** (1998) 014017.

[3] I. Balitsky, *Factorization for High-Energy Scattering*, *Phys. Rev. Lett.* **93** (1998) 2024–2027.

[4] Y. V. Kovchegov, *Small-x F_2 structure function of a nucleus including multiple Pomeron exchanges*, *Phys. Rev. D* **60** (1999) 034008; **61** (2000) 074018.

[5] J. L. Albacete, N. Armesto, J. G. Milhano, P. Quiroga Arias, and C. A. Salgado, *AAMQS: A non-linear QCD analysis of new HERA data at small-x including heavy quarks*, *Eur. Phys. J. C* **71** (2011) 1705.

[6] E. Iancu, K. Itakura, and S. Munier, *Saturation and BFKL dynamics in the HERA data at small-x*, *Phys. Lett. B* **590** (2004) 199-208.

[7] E. Iancu, K. Itakura, and S. Munier, *High-energy scattering of protons by nuclei*, *Nucl. Phys. B* **21** (1970) 135–157.

[8] A. H. Mueller, *Small x Behavior and Parton Saturation: A QCD Model*, *Nucl. Phys. B* **335** (1990) 115–137.